Why Does a Ga_2 Dimer React Spontaneously with H_2, but a Ga Atom Does Not?—A Detailed Quantum Chemical Investigation of the Differences in Reactivity Between Ga Atoms and Ga_2 Dimers, in Combination with Experimental Results

Andreas Köhn,[b] Hans-Jörg Himmel,*[a] and Benjamin Gaertner[a]

Abstract: The spontaneous and photoactivated reactions between Ga_2 and H_2 in a matrix of solid Ar at 12 K have been followed by using IR spectroscopy and have been shown to give access to several isomers of the subvalent hydride Ga_2H_2. We now present Raman spectra for this system, to complete its characterization on the basis of vibrational spectra. In addition, the differences between the reactivity of a Ga atom and a Ga_2 dimer toward H_2 are evaluated. The matrix isolation experiments have shown that Ga_2 reacts spontaneously with H_2, at 12 K, to give the cyclic subvalent hydride $Ga(\mu\text{-}H)_2Ga$ (D_{2h} symmetry), which can be transformed into two other isomers of Ga_2H_2 by selective photoactivation. Interestingly, the spontaneous reaction is subject to a marked isotopic effect. In total, the experimental results provide detailed information about the reaction mechanism. In contrast to Ga_2, Ga atoms do not react spontaneously with H_2; on photoactivation they instead yield the radical species GaH_2. The quantum chemical calculations presented herein start with an analysis of the structures and relative energies of the relevant species at the MP2 level, by using extended basis sets, and lead on to a discussion of the correlation diagrams for both reactions. Finally, CASSCF and MRCI methods, in combination with moderate-sized basis sets, were employed to analyze in detail the mechanisms of the two reactions. It will be shown that the computational results, in concert with the experimental findings, provide a satisfying explanation of the contrasting reactivities of Ga and Ga_2.

Keywords: ab initio calculations · gallium · hydrogen · Raman spectroscopy

Introduction

There is ongoing interest in metal clusters, stimulated mainly by the search for materials with new physical and chemical properties, for example, unusual electronic or magnetic behavior, or catalytic potential.[1] In this context, it has been shown in several cases that clusters exhibit characteristics that differ substantially from those of the bare atom on the one hand and those of the bulk on the other hand.[1] It is not only the physical but also the chemical properties that may show remarkable disparities. Despite the intense research in this field, not much is known about the reasons for such differences. This is because it is essential, in general, to have detailed and reliable knowledge of the potential-energy surface near the reaction coordinate relevant to the reaction under consideration—whatever parameter (distance or angle) this might be—to understand the contrasting behaviors. Unfortunately, this information is not easily acquired, often requiring very expensive calculations in addition to some hard experimental facts. The present study is concerned with gallium, for which several interesting new cluster compounds have been synthesized and characterized in the recent past.[1e] As a first step in the evaluation of the different reactivities of atoms and small clusters, consideration is given to the response of Ga atoms and the Ga_2 dimer to dihydrogen.

Recent experiments have shown[2, 3] that matrix-isolated Ga_2 dimers react spontaneously with H_2, at temperatures as low as 10 K, to give the doubly bridged species $Ga(\mu\text{-}H)_2Ga$ [reaction (1)], while Ga atoms do not react spontaneously under these conditions. Ga atoms instead require photoactivation through $^2S \leftarrow {}^2P$ or $^2D \leftarrow {}^2P$ excitation before inserting into the H–H bond with the formation of the Ga^{II} radical species GaH_2 [reaction (2)].[4, 5] However, both reactions are exothermic. Thus, a Ga atom carrying an unpaired electron in one of the frontier 4p orbitals, which one might intuitively expect to be more reactive than a Ga_2

[a] Dr. Dr. H.-J. Himmel, B. Gaertner
Institut für Anorganische Chemie der Universität Karlsruhe
Engesserstrasse, Geb. 30.45, 76128 Karlsruhe (Germany)
Fax: (+49) 721-608-4854
E-mail: himmel@chemie.uni-karlsruhe.de

[b] Dr. A. Köhn
Institut für Physikalische Chemie der Universität Karlsruhe
Fritz-Haber-Weg, Geb. 30.43, 76128 Karlsruhe (Germany)

 DOI: 10.1002/chem.200204633

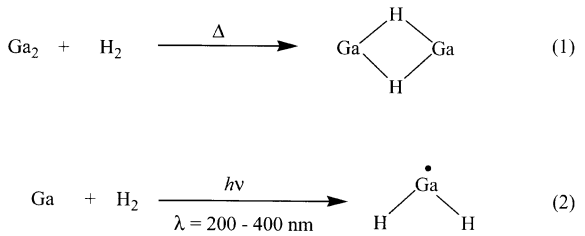

dimer, turns out to be relatively inert. The kinetic inertia of group 13 atoms appeared for a long time to be a teasing problem, for two reasons. Firstly, simple MO pictures tend to predict an attractive interaction between the half-filled frontier p orbital of the Group 13 atom and, for example, the σ* orbital of H_2. Secondly, the results of many experiments indicate that transition metal atoms are reactive not in their ground electronic state, but in an excited state corresponding to the excitation of an electron from a d orbital into an empty frontier p orbital.[6] We seek herein to offer a detailed and satisfying explanation of the conundrum presented by the different kinetic properties of Ga and Ga_2 vis-à-vis their reactions with H_2.

Additional motivation for the characterization of species such as Ga_2H_2 arises from the fact that subvalent hydrides of Group 13 elements are likely to play an important role in chemical vapor deposition (CVD) processes designed for the fabrication of thin metal or semiconductor coatings.[7] In these processes, a volatile compound containing the Group 13 element, for example, $Ga(CH_3)_3$, is decomposed near a surface, at elevated temperatures, in a stream of H_2, which may contain another species, such as NH_3.

Finally, a species like Ga_2H_2 is of considerable academic interest. This compound can adopt four isomeric forms, namely cyclic Ga(μ-H)$_2$Ga (D_{2h} symmetry), *trans*-bent HGa-GaH (C_{2h} symmetry), $GaGaH_2$ (C_{2v} symmetry) and Ga(μ-H)GaH (C_s symmetry), which differ in their energies by not more than 60 kJ mol^{-1}, according to quantum chemical calculations. The Ga–Ga bond in one of these isomers, the *trans*-bent species HGaGaH, is of particular interest, and much effort has been put into the synthesis of some of its derivatives with the formula RGaGaR′ (whereby R and R′ are sterically demanding organic groups). The first compound of this type (R = R′ = 2,6-Dipp$_2$C$_6$H$_3$, Dipp = 2,6-*i*Pr$_2$C$_6$H$_3$) has been structurally analyzed only very recently.[8]

Computational Methods

The nonrelativistic ab initio quantum chemical calculations relied on the Møller–Plesset second-order treatment of electron correlation by using the resolution of the identity approximation for fast integral transformation (RI-MP2), as implemented in the TURBOMOLE package.[9] Basis sets of triple zeta valence (TZV) quality developed by Ahlrichs and co-workers[10] were used in conjunction with appropriate sets of polarization functions. For gallium, only one primitive (2d1f) set, optimized for correlation of the valence electrons, is available (see ref. [11]), which has the short notation TZVPP. For inclusion of d-electron correlation, the underlying TZV basis was decontracted in the d-shell, giving a contraction pattern of (842111/63111/411) and yielding triple zeta quality for this shell also. An additional primitive (2f1g) set of polarization functions (exponents: 7.2, 2.0, and 5.0) was roughly optimized for correlation of the d electrons. This newly created basis set will be denoted TZVPPext in the following account. An auxiliary basis set, as required for RI-MP2, was optimized for this basis set and is available in electronic form from one of the authors (A.K.).[12] RI-MP2 and MP2 results differ by less than 1 kJ mol^{-1} in the case of reaction energies, less than 5 cm^{-1} in the case of vibrational frequencies, and less than 0.0001 Å for structural parameters. Geometry optimizations were carried out using analytic gradients, and vibrational properties were obtained by numerical differentiation.

To investigate the reaction path, we employed the CASSCF method, as implemented in the DALTON program package,[13] in combination with split valence plus polarization (SVP) basis sets.[14] All configurations allowed by distributing all valence electrons among the orbitals originating from gallium 4s and 4p and hydrogen 1s levels were included in the active space (full valence CAS). At this level of theory we carried out full and constrained geometry optimizations, as well as calculations of the vibrational frequencies. For optimizations in which certain selected coordinates were frozen, a Karlsruhe version of the DALTON code was used. For the single-reference-dominated minimum structures, the quality of the CASSCF description was assessed by comparison with the MP2 results. Near the transition state, multireference configuration interaction (MRCI) calculations were employed to analyze correlation effects, which include single and double excitations from the CAS into the secondary (or virtual) orbital space. For the non-size-consistent MRCI model, all relative energies are quoted relative to a Ga_2–H_2 "super-molecule", which consists of Ga_2 and H_2 (both in their ground electronic states) separated by 50 Å. For the CASSCF and MRCI calculations, we neglected the correlation of d electrons due to computational restrictions, although, as discussed later, this might affect any quantitative description. On the other hand, the level of theory employed should be sufficient to allow for a reasonable qualitative description of the electronic states relevant to the Ga/H_2 and Ga_2/H_2 reactions.

Experimental Section:

Details of the matrix isolation methods can be found elsewhere.[3] Very briefly, Ga vapor was co-deposited over a period of 2 hours with H_2, in an excess of Ar, on a freshly polished Cu block, which was kept at 12 K by means of a closed-cycle refrigerator (Leybold LB 510). The resulting matrix was characterized by its IR and Raman spectrum. The matrix was then subjected to several cycles of photolysis, and the changes thus brought about were monitored again by IR and Raman measurements. The experiments were repeated with different isotopomers (D_2 and HD).

The IR spectra were recorded with the aid of a Bruker 113v spectrometer, which allowed for measurements in the 4000–200 cm^{-1} region (MCT and DTGS detectors) with a resolution of 1 cm^{-1}. Raman spectra were recorded with the aid of a Dilor XY800 spectrometer equipped with a CCD camera (Wright Instruments, Si-chip from EEV). Both the $\lambda = 488$ nm and $\lambda = 514$ nm lines of an Ar-ion laser (Coherent, Innova 90-5) were used for excitation.

Results and Discussion

We start with a summary of the experimental findings which give detailed information about the reaction mechanisms to be analyzed by the subsequent quantum chemical calculations.

Matrix experiments: A full account of our experimental IR results can be found elsewhere.[3] We now present Raman spectra to complete the characterization of this system by vibrational spectroscopy. The rate of deposition of Ga was determined, by using a microbalance, to be 5 μg h^{-1}. A typical Raman spectrum recorded for a matrix containing up to 5% of H_2 in Ar, immediately after deposition, is shown in Figure 1. It contains two strong and sharp signals at 353.1

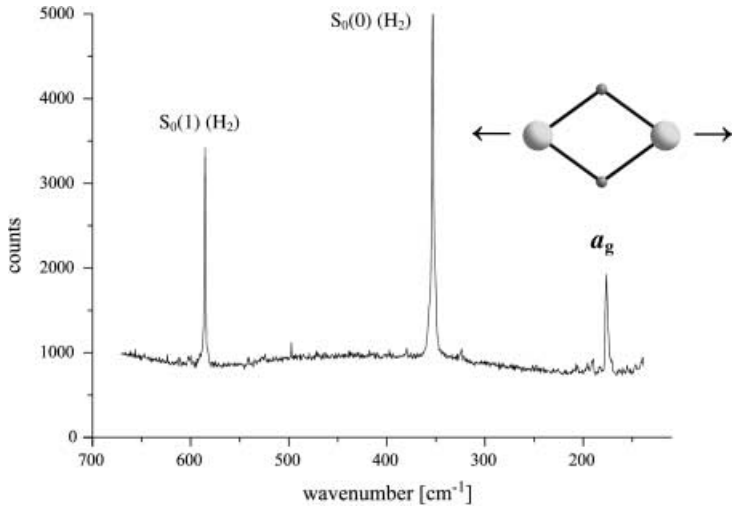

Figure 1. Raman spectrum taken upon deposition of Ga_2 together with H_2 in an excess of Ar.

and 585.3 cm^{-1}, which can be assigned to the rotational bands $S_0(0)$ and $S_0(1)$ of H_2 (notation $S_R(J)$, whereby S means $\Delta J = 2$ and $J = 0$ and 1, respectively, and R refers to a possible translational sideband of the pure transition). These bands originate from isolated H_2 molecules that are trapped in a matrix site free of Ga_2.[15] In addition to these features, a signal appeared at 176.2 cm^{-1}. This can be assigned to the $\nu_2(a_g)$ mode of Ga(μ-H)$_2$Ga. A combination mode $\nu_2(a_g) + \nu_4(b_{1u})$ had already been detected in the IR spectra and on this basis the wavenumber of the $\nu_2(a_g)$ mode was estimated to be 175 $\pm$ 5 cm^{-1}. Thus the IR and Raman results are in excellent agreement. The $\nu_2(a_g)$ mode can be described as a combination of the bending mode δ(H-Ga-H) and, if there is any interaction between the Ga atoms at all, Ga–Ga "stretching". The Raman experiment was repeated with D_2 in place of H_2. In these experiments, strong signals were observed at 178.6 and 296.8 cm^{-1} due to the rotational bands $S_0(0)$ and $S_0(1)$ of D_2. Appearing as a shoulder of the emission at 178.6 cm^{-1} was another sharp, strong signal at 176.1 cm^{-1}, which belongs almost certainly to the corresponding $\nu_2(a_g)$ mode of Ga(μ-D)$_2$Ga. The small shift of only 0.1 cm^{-1} of this mode upon H/D substitution is in good agreement with the predictions of quantum chemical calculations.[3] Unfortunately, because of fluorescence, our Raman experiments failed to detect the second a_1 and the b_{1g} mode of Ga(μ-H)$_2$Ga. The wavenumber of these modes can be estimated, on the basis of combination modes detected in the IR experiments, to be 1220 and 880 cm^{-1}, respectively.[3] Presumably because of the heat transferred into the matrix through the laser light, the Raman spectra gave immediate evidence of the formation of Ga(μ-D)$_2$Ga in case of Ga/D_2 mixtures. Both in the IR and the Raman experiments the bands belonging to Ga(μ-H)$_2$Ga decreased upon photolysis.

On the basis of the experimental results, normal coordinate calculations were performed on Ga(μ-H)$_2$Ga, for which five of the six vibrational fundamentals have been located experimentally. The four M–H bond lengths, the M···M separation, and the dihedral angle expressing the displacement of one atom relative to the plane defined by the other three (for out-of-plane motion), were chosen as internal coordinates. The wavenumbers for both M_2H_2 and M_2D_2 were employed to refine the force constants,[16] using experimental values where available. The force constant for elongation of the Ga···Ga separation was determined to be 97.8 N m^{-1}, very close to that of Ga_2, which is approximately 100 N m^{-1}.[19] However, this cannot be taken as clear evidence of interaction between the two Ga atoms in Ga(μ-H)$_2$Ga, as it is not possible to eliminate the contribution arising from Ga-H-Ga bending.

The matrix experiments conducted with Ga_2 dimers and Ga atoms proved that reactions (1) and (2), whether spontaneous or photoactivated, proceed in a concerted fashion.[3, 4] It follows that each reaction involves a one-step process for which a choice of reaction coordinates is indicated in Figure 2. In addition, extremely useful experimental information for the reaction of Ga_2 with H_2 is to hand. Figure 3 shows IR spectra recorded after deposition of Ga_2 together with Ar

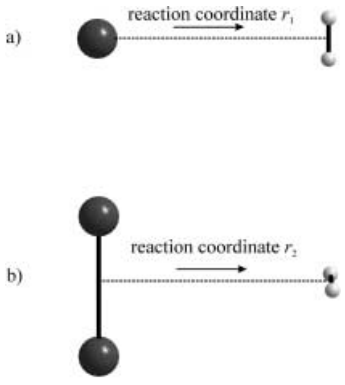

Figure 2. Definition of the reaction coordinates r_1 and r_2 for the reactions of H_2 with a) Ga to give GaH_2 and b) Ga_2 to give Ga(μ-H)$_2$Ga.

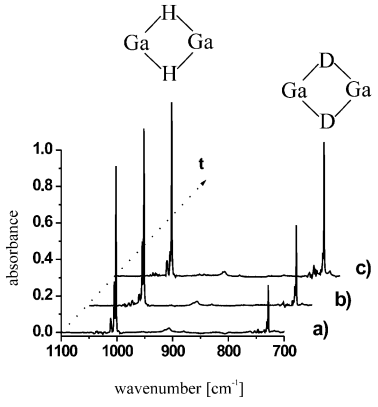

Figure 3. Infrared spectra in the region 1100–700 cm^{-1} recorded a) immediately after deposition of Ga vapor together with a 1:1 H_2/D_2 mixture in an excess of Ar (H_2/D_2/Ar = 0.4/0.6/100) at 14 K, b) after 12 hours, c) after 20 hours and exposure to IR light.

doped with an equimolar mixture of H_2 and D_2 at 14 K. The spectrum recorded immediately after deposition (Figure 3a) shows a very strong signal near 1002 cm^{-1}. This can be assigned to the $\nu_4(b_{2u})$ mode of singlet $Ga(\mu\text{-}H)_2Ga$,[3] which is formed spontaneously. On the other hand, it shows only a weak signal at 728 cm^{-1} due to the corresponding mode of $Ga(\mu\text{-}D)_2Ga$. Strikingly, however, the second signal has been observed to grow with time or if the matrix is exposed to IR radiation to provide slightly more energy. Hence, it appears that there is a small barrier to reaction. One possible explanation for this isotope effect is that there is a difference in the barrier heights for the systems Ga_2/H_2 and Ga_2/D_2 caused by differences in the zero-point energies of the reactants and/or the transition states. The second possibility is that the barrier is narrow enough to allow for effective tunneling through it, which is then subject to a marked isotopic effect.

Table 1. Dimensions [in Å], harmonic vibrational frequencies [in cm^{-1}] and relative energies [in kJ mol^{-1}] of Ga_2 in various electronic states, GaH, GaH_2, and Ga_2H_2.

			CASSCF/SVP	MP2/TZVPP	MP2/TZVPPext	Exptl.
Ga_2	$^3\Pi_u$	d(Ga–Ga)	2.763	2.714	2.632	
		ν(Ga–Ga)	161	178	188	180[18]
	$^3\Sigma_g^-$	ΔE	7.1	7.8	9.1	
		d(Ga–Ga)	2.510	2.471	2.394	
		ν(Ga–Ga)	204	222	238.4	
	$^1\Sigma_g^+$	ΔE	19.0	41.5	45.8	
		d(Ga–Ga)	3.093	3.003	2.915	
		ν(Ga–Ga)	121	146	153	
	$^1\Pi_u$	ΔE	46.3			
		d(Ga–Ga)	2.781			
		ν(Ga–Ga)	154			
	$^1\Delta_g$	ΔE	56.4			
		d(Ga–Ga)	2.587			
		ν(Ga–Ga)	170			
GaH	$^1\Sigma_g^+$	d(Ga–H)	1.700	1.679	1.651	
		ν(Ga–H)	1553	1653	1668	1513.8[4]
GaH_2	$^2A_1$	d(Ga–H)	1.623	1.596	1.562	
		$\sphericalangle$(H-Ga-H)	119.8	120.0	120.9	
		δ(H-Ga-H)	724	755	764	740.1[4]
		ν_s(Ga–H)	1743	1894	1927	1727.7[4]
		ν_{as}(Ga–H)	1993	1922	1967	1799.5[4]
Ga_2H_2	$^1A_1$	d(Ga–H)	1.892	1.871	1.836	
		d(H–H)	2.251	2.197	2.168	
		d(Ga–Ga)	3.042	3.029	2.964	
		$\nu(a_g)$	189	199	201	176.2 (this work)
		$\nu(b_{1u})$	292	303	282	
		$\nu(b_{3u})$	915	960	986	880[3b]
		$\nu(b_{1g})$	933	1011	1038	906.5[3b]
		$\nu(b_{2u})$	1136	1158	1162	1002[3b]
		$\nu(a_g)$	1278	1324	1341	1220[3b]

In summary, the experimental data give quite detailed information about the reaction mechanisms which will be used at several stages of the following quantum chemical analysis of the results. It should be noted that our calculations do not allow for any special matrix effects caused by the interaction of the molecules or atoms with the Ar atoms of the matrix cage.[17]

Quantum chemical calculations: Prior to the discussion of the reaction mechanisms, the structures and relative energies of the relevant electronic states of Ga_2, GaH_2, and Ga_2H_2 will be explored. For some species, there is information from experimental and/or previous quantum chemical studies, which provides tests of the accuracy of the methods and basis sets used later for the exploration of the potential-energy surfaces. There follows a discussion of the correlation diagrams for the systems Ga/H_2 and Ga_2/H_2, which afford useful qualitative information about the reactions. Finally, the potential-energy surfaces are analyzed for a detailed description of the reaction mechanism.

Ga_2, GaH_2 and Ga_2H_2 in their global energy minimum structures: Dimensions and harmonic frequencies calculated at different levels of theory are summarized in Table 1. Theory and experiment agree that Ga_2 assumes a triplet ground electronic state.[18–20] The lowest energy triplet valence-shell configuration ($\sigma_g^2\sigma_u^2\sigma_g^1\pi_u^1$) results in a $^3\Pi_u$ state with a Ga–Ga distance of 2.76 Å at the CASSCF/SVP level. MP2 theory gives a considerably shorter bond length (2.71 Å), which shrinks even further (to 2.63 Å) if the correlation of the d electrons ($d^{10}-d^{10}$ interaction) is taken into account. In addition, the $\sigma_g^2\sigma_u^2\pi_u^2$ configuration of the valence shell gives rise to the $^3\Sigma_g^-$ state (with a Ga–Ga distance of 2.39 Å at the MP2/TZVPPext level), which our calculations find to be only 7–9 kJ mol^{-1} more energetic than the $^3\Pi_u$ state (see Table 1). The singlet electronic state lowest in energy is $^1\Sigma_g^+$ with the valence-shell configuration $\sigma_g^2\sigma_u^2\sigma_g^2$ and a Ga–Ga distance of 2.92 Å (3.09 Å at the CASSCF level); this is calculated to lie 46 kJ mol^{-1} higher in energy than the $^3\Pi_u$ ground electronic state. The CASSCF calculation predicts, however, an adiabatic separation of not more than 19 kJ mol^{-1}, a result of some importance to the following discussion of possible reaction pathways. Two additional singlet electronic states, $^1\Pi_u$ and $^1\Delta_g$, might also be of importance; these have energies 46 and 56 kJ mol^{-1}, respectively, above the ground electronic state at the CASSCF level. As a general trend, we find the Ga–Ga distance shortens upon inclusion of dynamic electron correlation (by about 0.04–0.09 Å), an effect which is even more pronounced if the d-shells are correlated by using appropriately modified basis sets. Simultaneously, the vibrational frequencies increase by 20–30 cm^{-1} (see Table 1).

Table 2 includes the atomization and reaction energies of relevance to our analysis. The dissociation energy of Ga_2, including the harmonic estimate of the zero-point energy (ZPE), ranges from 92 to 131 kJ mol^{-1} for the different levels of theory employed. Our MP2/TZVPPext result may be corrected for the basis-set superposition error to give a value

Table 2. Reaction energies at 0 K [in kJ mol^{-1}, ZPE corrections included].

Reaction	CASSCF/SVP	MP2/TZVPP	MP2/TZVPPext	Exptl.
$H_2 \rightarrow 2H$	+366.2		+406.2	+432.07(1)[a]
$Ga_2 \rightarrow 2Ga$	+91.8	+117.7	+131.1	110.3(7.0)/110.8(4.9)[b]
$GaH \rightarrow Ga + H$	+248.3	+257.9	+260.9	<274[24]
$Ga + H_2 \rightarrow GaH + H$	+117.9	+148.3	+145.3	
$Ga + H_2 \rightarrow GaH_2$	−2.3	−15.9	−13.3	
$Ga_2 + H_2 \rightarrow Ga_2H_2$	−93.1	−95.7	−96.0	
$Ga_2H_2 \rightarrow 2GaH$	+54.4	+103.8	+111.5	

[a] JANAF Thermochemical Tables, 3rd ed., *J. Phys. Chem. Ref. Data* **1998**, *4*, Monograph 9. [b] See ref. [23].

of 124 kJ mol^{-1}. Spin-orbit contributions (estimated on the basis of earlier work[21]) reduce this value by another 9 kJ mol^{-1}. Overall, the value calculated here is in reasonable agreement with the experimental value of 110.8 ± 4.9 kJ mol^{-1}.[22, 23]

The calculated relative energies of the electronic states of Ga_2 are in fair agreement with the results of earlier MR-ACPF calculations,[20] which predicted the $^3\Sigma_g^-$, $^1\Sigma_g^+$, $^1\Pi_u$, and $^1\Delta_g$ states to lie 10.6, 34.7, 44.4, and 48.2 kJ mol^{-1}, respectively, above the energy of the $^3\Pi_u$ ground state. In this earlier work, the Ga–Ga separations and harmonic frequencies ν(Ga–Ga) of the $^3\Pi_u$, $^3\Sigma_g^-$, $^1\Sigma_g^+$, $^1\Pi_u$, and $^1\Delta_g$ states were calculated to be 2.69, 2.47, 2.94, 2.70, 2.55 Å, and 170, 210, 118, 169, 170 cm^{-1}, respectively.[20]

GaH possesses a closed-shell ground state ($^1\Sigma_g^+$). The bond length and the harmonic vibrational frequency are predicted to be 1.65 Å and 1668 cm^{-1}, respectively, in good agreement with the experimentally determined values of 1.6621 Å and 1604 cm^{-1}.[4, 24] It is evident from the values calculated with different methods and basis sets (see Table 1) that dynamic correlation and d-shell inclusion lead to further significant alterations in the values calculated for these observable parameters.

GaH_2 has been studied previously in inert gas matrices by means of IR and EPR spectroscopy.[4, 5] The experimental results clearly show that GaH_2 is a bent molecule with C_{2v} symmetry. On the basis of the experimental results, the H-Ga-H bond angle was estimated to be approximately 120°.[4] Previous calculations[25–27] predict an H-Ga-H bond angle and a Ga–H bond length of 118–120.4° and 1.580–1.616 Å, respectively. In delivering a Ga–H bond length of 1.56 Å and a H-Ga-H bond angle of 121°, our calculations are in good agreement with these previous reports. Trends similar to those discussed for Ga_2 and GaH are found if different levels of theory are applied (see Table 1).

As already mentioned, Ga(μ-H)$_2$Ga has been characterized on the basis of its IR spectrum.[3] The Ga–H and Ga···Ga distances of this planar molecule (D_{2h} symmetry) were calculated to be 1.84 and 2.96 Å, respectively, and the H-Ga-H angle was calculated to be 72.4°. Again, our values are in good agreement with those obtained previously by applying DFT or CCSD methods,[3, 27–29] although the bond lengths are significantly shorter in our calculations, probably because of the inclusion of d^{10}–d^{10} interactions. We note further that the Ga···Ga separation in Ga(μ-H)$_2$Ga is close to the value adopted for Ga_2 in its $^1\Sigma_g^+$ electronic state. In the following discussion, we will see that the reaction of Ga_2 with H_2 (along the reaction coordinate r_2 as defined in Figure 2) involves first a shortening and then a lengthening of the Ga···Ga separation.

Correlation diagrams: The experimental results favor concerted reaction mechanisms for both Ga + H_2 and Ga_2 + H_2. It will be shown in the following discussion that the choice of high-symmetry coordinates as defined in Figure 2 is reasonable, and that the C_{2v} symmetry is maintained throughout the reactions. The correlation diagrams for the systems Ga/H_2 and Ga_2/H_2 are visualized in Figures 4 and 5. In the case of the reaction of atomic Ga with H_2, the initial valence-shell electronic configuration is $\sigma^2 4s^2 4p^1$, which translates into the three possible valence-shell configurations $a_1^2 a_1^2 a_1^1$, $a_1^2 a_1^2 b_1^1$, and $a_1^2 a_1^2 b_2^1$ for an approach of the two reactants in C_{2v} symmetry. However, according to our simple correlation diagram, none of these three configurations leads to the ground-state valence-shell electronic configuration of the GaH_2 product, which is $a_1^2 b_1^2 a_1^1$. Instead, the valence-shell configurations lead to excited states of GaH_2.[30] In the case of the reverse process, the decomposition of GaH_2 into a Ga atom and H_2, the valence-shell configuration $a_1^2 b_1^2 a_1^1$ prior to decomposition correlates with an electronic configuration $\sigma^2 4s^1 4p^2$ for the Ga atom after decomposition. This might imply that a $^2D \leftarrow {}^2P$ or $^2S \leftarrow {}^2P$ electronic excitation of the Ga atom would support the forward reaction, and in fact it has

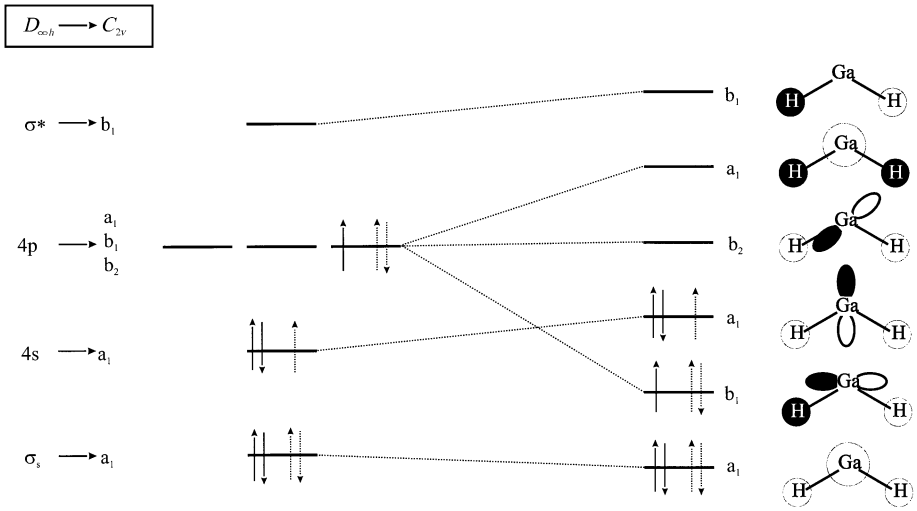

Figure 4. Correlation diagram for the reaction between a Ga atom and H_2 to give HGaH [reaction (2)].

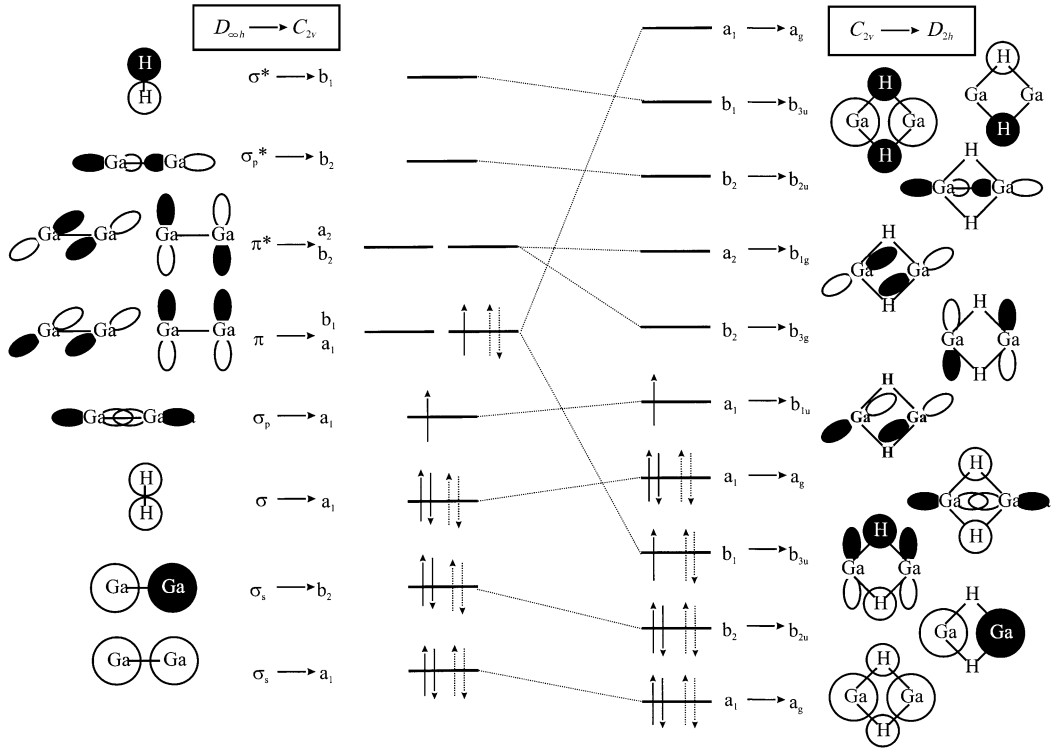

Figure 5. Correlation diagram for the reaction between a Ga_2 dimer and H_2 to give Ga_2H_2 [reaction (1)].

been reported that Ga atoms in their ^2D (and also ^2S) electronic state react spontaneously with H_2 to give GaH_2.[4, 5]

Figure 5 shows the corresponding correlation diagram for the reaction of Ga_2 with H_2 to give $Ga(\mu\text{-}H)_2Ga$. The $\sigma_g^2\sigma_u^2\sigma_g^2\sigma_g^1\pi_u^1$ ground-state valence-shell configuration translates into $a_1^2b_2^2a_1^2a_1^1a_1^1$ or $a_1^2b_2^2a_1^2a_1^1b_1^1$ configurations in C_{2v} symmetry. $Ga(\mu\text{-}H)_2Ga$ in D_{2h} symmetry exhibits a ground electronic state with the valence-shell configuration $a_g^2b_{2u}^2b_{3u}^2a_g^2$, which corresponds to $a_1^2b_2^2b_1^2a_1^2$ in C_{2v} symmetry. From Figure 5 it is clear that neither of the two possible initial electronic states will lead to this ground electronic state. The $\sigma_g^2\sigma_u^2\sigma_g^2\sigma_g^1\pi_u^1$ valence-shell electronic state of Ga_2 leads instead to the excited electronic state of $Ga(\mu\text{-}H)_2Ga$ with the configuration $a_g^2b_{2u}^2b_{3u}^1a_g^2b_{1u}^1$. On the other hand, decomposition of $Ga(\mu\text{-}H)_2Ga$ into Ga_2 and H_2 would, according to our diagram, lead to Ga_2 in its $^1\Delta_g$ or $^1\Sigma_g^+$ electronic state, but not of course directly to the $^3\Pi_u$ ground state.

In summary, the correlation diagrams show that the reactions of H_2 with both Ga and Ga_2 feature electronic states of the reactants that are incompatible with those of the products, and, therefore, there must be a change of electronic state somewhere along the reaction coordinate. This change also brings with it the expectation of at least a small barrier that has to be overcome if the reactions are to take place.

Reaction mechanisms

Ga + H_2: The reaction energy for reaction (2) was calculated to be $-13\,kJ\,mol^{-1}$ at the MP2 level of theory. This implies that the Ga–H bond formation can only just compensate for the large energy required to break the H_2 bond. The CASSCF calculation yields a somewhat smaller value of $-2\,kJ\,mol^{-1}$. As a first step, calculations were employed to analyze the approach of a Ga atom to an H_2 molecule along a high-symmetry C_{2v}-symmetric path (reaction coordinate r_1, see Figure 2), leading to a concerted reaction. Figure 6 shows the potential energy, defined relative to that of a Ga atom in its ^2P ground electronic state and an H_2 molecule at infinite separation, as a function of the reaction coordinate r_1. For

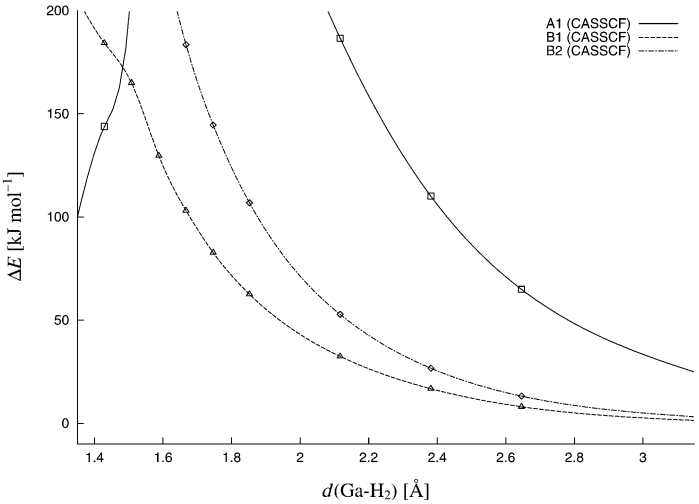

Figure 6. CASSCF potential energy for the approach of Ga and H_2 along the high-symmetry path (C_{2v}, see Figure 1). Shown are the three states arising from the degenerate ^2P state of Ga. At each value of r_1, the remaining dimensions were optimized for the $^2B_1$ electronic state at the CASSCF level.

all electronic states arising from ^2P ($^2A_1$, $^2B_1$, and $^2B_2$), the potential energy increases rapidly for values of r_1 smaller than 2.0–2.5 Å. The potential-energy curve of the $^2B_1$ state, for which the singly-occupied Ga 4p orbital is oriented parallel to the H_2 axis, exhibits the smallest energy increase. For symmetry reasons, however, this state evidently does not lead directly to the desired product. The $^2A_1$ state, which is initially highly repulsive, does not change much if the H–H distance for this state is optimized. An inspection of the second derivatives of the potential energies shows that the vibrational modes which break the C_{2v} symmetry exhibit imaginary wavenumbers for this state, indicating that another reaction path is energetically favored. Additionally, we note that at $r_2 < 2$ Å the $^2B_1 - ^2A_1$ separation decreases again and at $r_1 <$ 1.45 Å the $^1A_1$ state becomes lower in energy than the $^2B_1$ state. At these distances the $^1A_1$ state already has the product configuration ($a_1^2b_1^2a_1^1$). Hence we may conjecture that reduction of the symmetry will lead to a neighboring transition state that connects the reactant and product potential-energy surfaces. Our calculations do indeed suggest a low symmetry, but now nonconcerted, reaction pathway, proceeding in two steps, first to the simple Ga^I hydride GaH and H atom and then, on recombination, to the GaH_2 product [reactions (3) and (4)].[31]

$$Ga + H_2 \rightarrow GaH + H^{\cdot} \quad (3)$$

$$GaH + H^{\cdot} \rightarrow HGa^{\cdot}H \quad (4)$$

Our CASSCF calculations result in a reaction energy (including ZPE) of $+118\ kJ\,mol^{-1}$ for the first step leading to GaH and H; MP2 calculations predict a somewhat larger value of $+145\ kJ\,mol^{-1}$. The endothermic character of the reaction testifies to the weakness of the newly formed Ga–H bond formed at the expense of the strong H–H bond. At $+138\ kJ\,mol^{-1}$ (including ZPE), the CASSCF reaction barrier for this first step comes out to be only slightly higher than the reaction energy. The second step, leading to the GaH_2 reaction product, is exothermic by $-120\ kJ\,mol^{-1}$ ($-159\ kJ\,mol^{-1}$ at the MP2 level); according to our CASSCF calculations, it is opposed by a minuscule barrier with a height not exceeding $+4\ kJ\,mol^{-1}$. Figure 7 is designed to illustrate this reaction pathway and the geometries of the transition states.

Ga_2 + H_2: According to our calculations, reaction (1) is exothermic by some $-96\ kJ\,mol^{-1}$ at the MP2/TZVPPext level; the CASSCF/SVP result is $-93\ kJ\,mol^{-1}$. As already mentioned, several electronic states of Ga_2 have to be taken into account. In principle, three mechanisms have then to be considered (see Scheme 1).

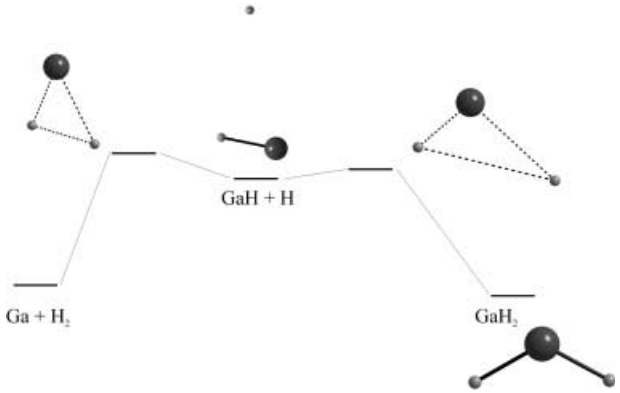

Figure 7. Schematic representation of the reaction of Ga and H_2 leading to GaH_2 along the low-symmetry path (C_s).

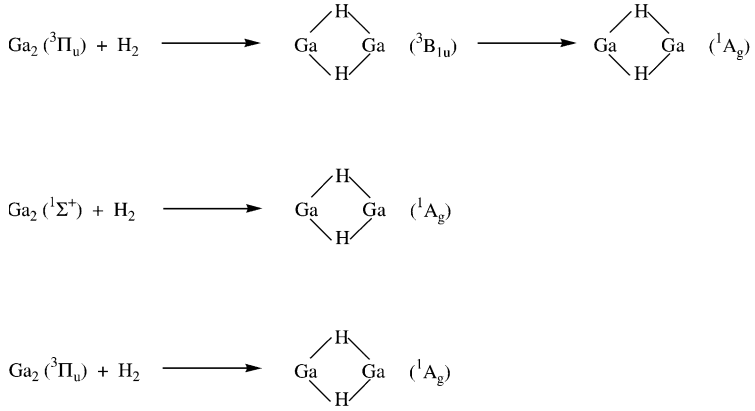

Scheme 1. Illustration showing the three possible mechanisms for the reaction of Ga_2 dimers with H_2 to give $Ga(\mu\text{-}H)_2Ga$.

1) Reaction occurs between Ga_2 in a triplet electronic state and H_2 to give $Ga(\mu\text{-}H)_2Ga$ in an excited triplet electronic state (Scheme 1, top). In a second step, this species is quenched (e.g., by the matrix environment or in the gas phase by collision with a third body), to deliver $Ga(\mu\text{-}H)_2Ga$ in its singlet ground electronic state.
2) The process starts with the excitation of Ga_2 from its triplet ground state into its lowest energy singlet state (Scheme 1, middle). This is a "forbidden" process that might, nevertheless, be brought about by spin-orbit coupling, which is already significant for Ga_2 (giving a maximum splitting of the $^3\Pi_u$ level that amounts to about 470 cm^{-1}[21]), and with the aid of the environment. This intersystem crossing is then followed by reaction with H_2 to give singlet $Ga(\mu\text{-}H)_2Ga$.
3) A third possibility begins with a triplet Ga_2/H_2 system and ends with a singlet $Ga(\mu\text{-}H)_2Ga$ product by way of an intersystem crossing somewhere on the reaction coordinate (Scheme 1, bottom). This triplet–singlet electronic transition can again be achieved either through spin-orbit coupling or, in a solid noble gas matrix, through the potential of the matrix environment to contain and efficiently quench excited molecular species.[17]

In the following account, we discuss these three possible reaction mechanisms. We start again by assuming the

symmetry of the approaching molecules to be C_{2v} for all values of the reaction coordinate r_2. This assumption makes sense on the basis of the experimental findings, which support a concerted reaction pathway. It also emerges, from an inspection of the second derivatives of the potential energies, that none of the vibrational modes that break the C_{2v} symmetry exhibit imaginary wavenumbers, implying that we have indeed chosen the lowest energy path.

At the stage of the approach of H_2 toward Ga_2, when the two reactants can no longer be treated as separated molecules, the overall symmetry is C_{2v} and the degenerate $^3\Pi_u$ state of Ga_2 splits into two states: a $^3B_1$ (component perpendicular to the reaction coordinate r_2) and a $^3A_1$ (component collinear with r_2) state. Of these two states the $^3B_1$ state is energetically favored. Figure 8 shows the potential energy of Ga_2/H_2 in its

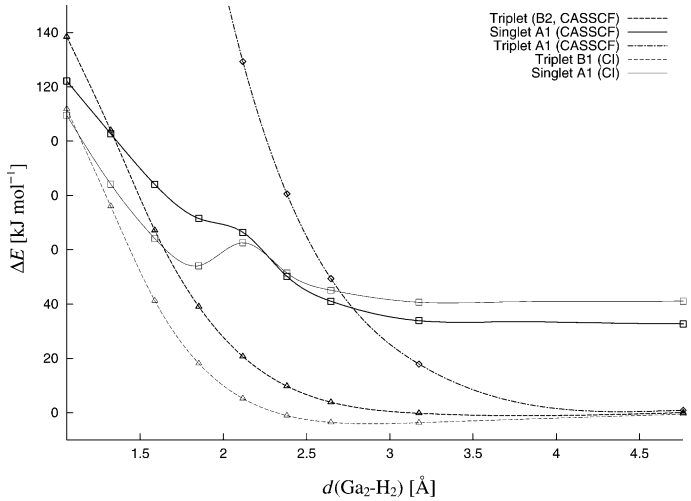

Figure 8. CASSCF (bold lines) and MRCI (thin lines) potential energy in dependence of r_2 (see Figure 1 for its definition) for the approach of Ga_2 and H_2 along the high-symmetry path (C_{2v}). At each value of r_2, the remaining dimensions were optimized for the $^3B_1$ state at the CASSCF level.

$^3B_1$ electronic state as a function of r_2; at each point the H···H and Ga···Ga separations were optimized at the CASSCF level. The potential energy is expressed relative to the energy at infinite separation of the Ga_2 ($^3\Pi_u$) and H_2 molecules. It is evident from Figure 8 that a significant repulsive interaction between H_2 and Ga_2 starts for values of r_2 smaller than about 3 Å. If correlation is included, a significant interaction starts at somewhat smaller values of r_2.

An additional curve in Figure 8 represents the relative energies of the $^3A_1$ electronic state of the Ga_2/H_2 system, with the energies calculated at each value of r_2 for the same geometries as for the $^3B_1$ state. In this case the repulsive interaction between the H_2 and Ga_2 molecules starts at a much earlier stage than it does for the $^3B_1$ electronic state. A repulsion energy amounting to 50 kJ mol^{-1} has already been reached at $r_2 \approx 2.7$ Å and exceeds 150 kJ mol^{-1} at $r_2 = 2$ Å. This behavior does not change significantly if the geometry of the $^3A_1$ state is fully optimized. On these grounds it can be argued that the $^3A_1$ electronic state is unlikely to play a major role in the reaction mechanism, although it would lead directly to the $^3B_{1u}$ excited state of Ga(μ-H)$_2$Ga. The situation resembles that of the Ga + H_2 system ($^2B_1$ and $^2A_1$ states), and we likewise expect the reaction leading to the lowest energy triplet electronic state of Ga(μ-H)$_2$Ga to occur after symmetry breaking in a nonconcerted fashion. From our calculations, the barrier height can be estimated to exceed 120 kJ mol^{-1}. Accordingly, we can rule out such a mechanism.

Finally, Figure 8 shows how the relative potential-energy curve derived for the $^1A_1$ electronic state, which represents the lowest energy singlet electronic state, varies with r_2. Due to the energy difference between the $^3\Pi_u$ and $^1\Sigma_g^+$ electronic states of Ga_2, the energy for the $^1A_1$ state at infinite values of r_2 is 19 kJ mol^{-1} higher than that calculated for the $^3B_1$ state. This singlet–triplet separation is somewhat smaller when calculated at the CASSCF level than at the correlated level (46 kJ mol^{-1} at the MP2/TZVPP and 32 kJ mol^{-1} at the MRCI/SVP level). However, both CASSCF and MRCI calculations agree that the singlet state shows a much smaller repulsive interaction, upon approach of the reactants, than do the other electronic states, and for $r_2 < 1.482$ Å the $^1A_1$ state becomes energetically favored.

Figure 9a shows the potential-energy surface as calculated for the $^1A_1$ electronic state using CASSCF/SVP. In this representation, the energy is plotted as a function of the reaction coordinate r_2 and the H–H separation, and the Ga–Ga distance is optimized at the CASSCF level at each point. For values of r_2 larger than 1.8 Å, the H–H bond still remains intact, but it breaks upon passing the transition state at $r_2 = 1.6$ Å and relaxes to a H···H separation close to the one finally adopted in the Ga(μ-H)$_2$Ga molecule. The transition state was also explicitly optimized at the CASSCF level and found to possess a single imaginary frequency. The "classical" barrier to reaction (not accounting for possible tunneling processes) amounts to about 53 kJ mol^{-1} (relative to $H_2 + Ga_2(^1\Sigma_g^+)$) without ZPE and does not change significantly after ZPE corrections (minuscule change to 52 kJ mol^{-1}).[32] It follows that the isotope effects for such a mechanism should be rather small. Indeed, for the corresponding reaction of Ga_2 with D_2 to give Ga(μ-D)$_2$Ga, we calculate a barrier only 0.5 kJ mol^{-1} higher. Relative to the triplet ground electronic state of Ga_2, the "classical" barrier height then amounts to about 70 kJ mol^{-1}.

To assess the influence of dynamic correlation, the calculations were repeated at the MR-CI level. The results of these calculations are depicted in Figure 10. As already pointed out, the calculations result in a larger singlet–triplet gap (32 kJ mol^{-1}), but the barrier height on the singlet hypersurface now amounts to only 19 kJ mol^{-1}, giving an overall "classical" barrier height of 51 kJ mol^{-1} relative to the triplet ground state. A comparison of Figures 9a and 10a reveals only minor changes in the topology of the energy surface.

The barrier is also relatively broad and therefore efficient tunneling, accompanied by what is likely to be a significant isotopic effect, is not expected to take place. However, the computational results indicate that the reaction, if it follows this pathway, has to proceed through the transition state and so has to overcome the full "classical" barrier height.

We finally come to a discussion of the potential-energy surface as calculated for the $^3B_1$ electronic state, the energy

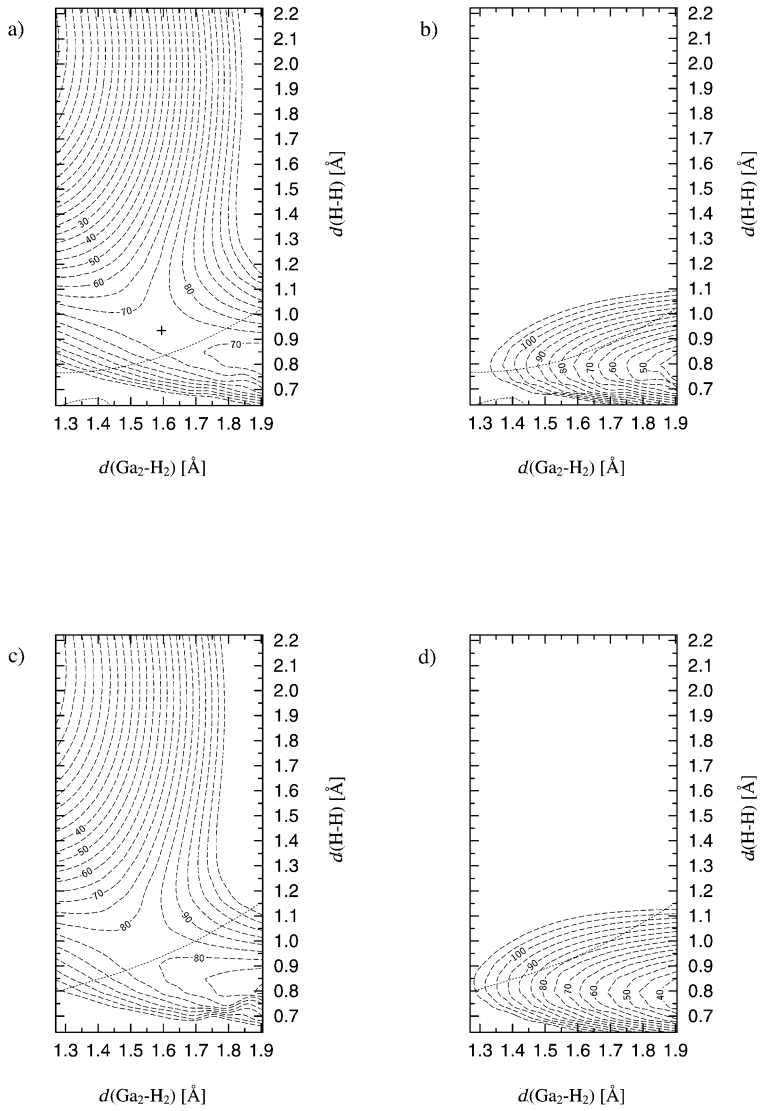

Figure 9. CASSCF potential-energy surfaces for the high-symmetry path (C_{2v}). a) $^1A_1$ electronic state with relaxed Ga–Ga distances; the position of the TS is marked by a cross. b) $^3B_1$ electronic state at the Ga–Ga distances relaxed for $^1A_1$; the dotted line indicates the intersection of the surfaces a) and b). c) $^1A_1$ electronic state at the Ga–Ga distances relaxed for $^3B_1$. d) $^3B_1$ electronic state with relaxed Ga–Ga distances; the dotted line indicates the intersection of the surfaces c) and d).

again being expressed as a function of the reaction coordinate r_2 and the H···H separation (with the Ga···Ga distance optimized at the CASSCF level). The results at the CASSCF and MRCI levels are monitored in Figures 9d and 10d, respectively. In order to find the intersection between the potential-energy curves for the $^1A_1$ and $^3B_1$ electronic states, we have calculated additionally at each point the energy of the $^1A_1$ electronic state, the geometry being the same as for the $^3B_1$ electronic state at this point. Hence, we have determined the vertical singlet–triplet separations between the two potential-energy surfaces. The surfaces, displayed in Figures 9c and 10c, reveal only small differences in comparison with the relaxed surfaces, which are plotted in Figures 9a and 10a, respectively. The intersection line, along which the singlet and triplet electronic states are degenerate, is also shown. Similarly, for the relaxed $^1A_1$ surface the $^3B_1$ energy at each point was calculated, with the results displayed in Figures 9b and 10b.

At the CASSCF level, the singlet–triplet intersection has its minimum close to the values of r_2 and d(H–H) adopted in the transition state on the singlet surface. The energy at this point is 80 kJ mol^{-1} and thus 10 kJ mol^{-1} higher than the energy of the transition state, which is reached by relaxation of the Ga···Ga distance towards its singlet equilibrium distance. The intersection between the relaxed $^1A_1$ state and the triplet state occurs at about 70 kJ mol^{-1}. However, the intersection takes place shortly before the transition state on the $^1A_1$ surface is reached (see Figure 9a/b). A similar result is obtained at the MRCI level: the singlet–triplet intersection reaches its minimum at $r_2 = 1.53$ Å and d(H–H) = 0.95 Å, and has an energy about 65 kJ mol^{-1} higher than that of the reactants and 15 kJ mol^{-1} higher than that of the transition state on the singlet surface. As with the results of the CASSCF calculations, the relaxed $^1A_1$ state intersects already at $r_2 = 1.65$ Å with a minimum energy of about 50 kJ mol^{-1}. Computational restrictions prevented us from calculating the spin-orbit-induced interaction potential between the $^3B_1$ and $^1A_1$ potentials. Nevertheless, we note that the spin-orbit interaction can mix the two states (in other words, $^3B_1$ and $^1A_1$ states map to the same irreducible representation of the C_{2v} double group and therefore, in a relativistic treatment, both states possess the same symmetry).

Though the energetics alone do not clearly favor the mechanism shown at the bottom of Scheme 1, there is a kinetic aspect which makes this mechanism the candidate most likely to explain the experimental findings. It has been argued earlier that the second mechanism (Scheme 1, middle) is not expected to show a strong isotope effect. Tunneling processes also seem unlikely to be of significance because of the relatively broad barrier. If, on the other hand, we inspect the topology of a composite potential-energy surface consisting of the triplet state (Figures 9d or 10d, respectively) on one side and the singlet state (see Figures 9a and 10a) on the other side of the intersection line, we find that the barrier width is much reduced, making tunneling a likely process. A pronounced isotope effect may than be expected, in agreement with the experimental findings.

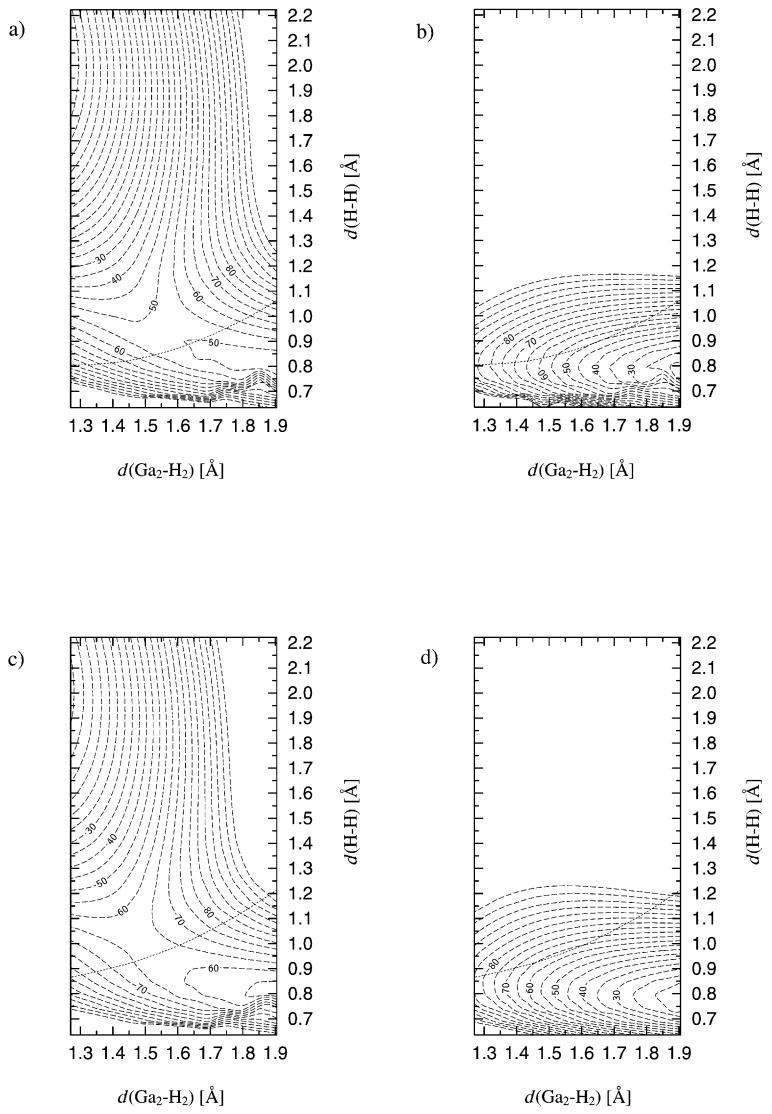

Figure 10. MRCI potential-energy surfaces for the high-symmetry path (C_{2v}). a) $^1A_1$ electronic state with relaxed Ga–Ga distances (optimized at the CASSCF level). b) $^3B_1$ electronic state at the Ga–Ga distances relaxed for $^1A_1$; the dotted line indicates the intersection of the surfaces a) and b). c) $^1A_1$ electronic state at the Ga–Ga distances relaxed for $^3B_1$. d) $^3B_1$ electronic state with relaxed Ga–Ga distances; the dotted line indicates the intersection of the surfaces c) and d).

An interesting point of the analysis is that the Ga···Ga separation first decreases and then increases again in the course of the reaction between Ga_2 and H_2. This behavior can be understood from an analysis of the wavefunctions. In the course of the approach of the two reactants, the $^3\Pi_u$ and $^3\Sigma_g^-$ type states of the Ga_2 moiety mix and the optimal Ga–Ga distance is about 2.65 Å. At the point of intersystem crossing from triplet to singlet states, Ga_2 adopts a $^1\Delta_g$-type state for which the optimal distance is somewhat shorter (about 2.55 Å). After the intersystem crossing, the Ga–Ga distance again increases, and the ground electronic state of the product reflects the $^1\Sigma_g^+$ state of Ga_2, with its Ga–Ga distance of about 3.00 Å.

In summary, the calculations favor the third mechanism (Scheme 1, bottom), which includes, firstly, the approach of the fragments on the triplet surface, followed by an intersystem crossing. According to our MRCI calculations, the barrier height for reaction (1) amounts to 50 – 60 kJ mol^{-1}, which is somewhat higher than the value of 35 kJ mol^{-1} estimated on the basis of the experimental results.[3] Clearly, in view of the modest basis set and the neglect of semi-core d-electron correlation, no quantitative prediction is to be expected on the basis of these calculations. However, the third mechanism suggests a significant contribution from tunneling, which is in accord with the experimentally observed isotope effects. What can definitely be concluded is that reaction (1) is opposed by a much lower barrier than reaction (2). The calculations therefore succeed in correctly predicting the differences in reactivity between a Ga atom and a Ga_2 dimer.

Conclusion

In summary, the results of this study, which are based on experimental facts as well as detailed quantum chemical calculations, offer a satisfactory explanation of the striking differences in reactivity, with respect to H_2, displayed by a Ga atom and a Ga_2 dimer under conditions of matrix isolation. The barriers to reaction with H_2 found in this study are characterized and can be attributed to changes of electronic state (rehybridization). In other words, what makes Ga_2 more reactive than Ga is its access to a greater range of excited electronic states at relatively low energies; moreover, the specific characters of these states, with their associated orbital symmetries and multiplicities, is likely also to make Ga_2 more *selective* in its reactions. The barriers to the reactions of Ga atoms, in their ^2P ground electronic state to give doublet GaH_2, and of Ga_2 molecules, in their $^3\Pi_u$ ground electronic state to give triplet Ga(μ-H)$_2$Ga, are too high for the reactions to occur spontaneously. In the case of Ga/H_2, the calculations predict, for the thermal reaction, a radical mechanism leading first to GaH + H and then to GaH_2. On the other hand, the reaction of Ga_2 molecules in the $^3\Pi_u$ ground electronic state with H_2 to form singlet Ga(μ-H)$_2$Ga, with an intersystem crossing during the approach, is subject to only a small activation barrier. The analysis of the barrier structure suggests that efficient

tunneling processes may occur and, thus, account satisfactorily for the significant isotope effect revealed by experiment.[3] It is likely, too, that the same factors, namely rehybridization effects, which dictate the reactivity patterns of the Ga atom versus the Ga_2 dimer, also play key roles in governing the reactivities of larger gallium clusters. In this sense, the present study is a small step towards a better understanding of the chemical properties of clusters, which can be very different from those of not only the corresponding atoms, but also the bulk metal.

Acknowledgements

The authors thank Prof. R. Ahlrichs for fruitful discussions and support, and the Deutsche Forschungsgemeinschaft for financial support, partially through SFB 195 ("Lokalisierung von Elektronen in mikroskopischen und makroskopischen Systemen") and the award of a Habilitanden-Stipendium (to H.-J.H.).

[1] See, for example: a) B. C. Gates, *Chem. Rev.* **1995**, *95*, 511; b) J. Evans, *J. Chem. Soc. Dalton. Trans.* **1996**, 555; c) A. Ecker, E. Weckert, H. Schnöckel, *Nature* **1997**, *287*, 379; d) B. F. G. Johnson, *Coord. Chem. Rev.* **1999**, *190–192*, 1269; e) H. Schnöckel, A. Schnepf, *Adv. Organomet. Chem.* **2001**, *47*, 235.

[2] Z. L. Xiao, R. H. Hauge, J. L. Margrave, *Inorg. Chem.* **1993**, *32*, 642.

[3] a) H.-J. Himmel, L. Manceron, A. J. Downs, P. Pullumbi, *Angew. Chem.* **2002**, 41, 796; *Angew. Chem. Int. Ed.* **2002**, *114*, 829; b) H.-J. Himmel, L. Manceron, A. J. Downs, P. Pullumbi, *J. Am. Chem. Soc.* **2002**, *124*, 4448.

[4] P. Pullumbi, C. Mijoule, L. Manceron, Y. Bouteiller, *Chem. Phys.* **1994**, *185*, 13.

[5] L. B. Knight Jr., J. J. Banisaukas III, R. Babb, E. R. Davidson, *J. Chem. Phys.* **1996**, *105*, 6607.

[6] See, for example: a) S. C. Chang, R. H. Hauge, W. E. Billups, J. L. Margrave, Z. H. Kafafi, *Inorg. Chem.* **1988**, *27*, 205; b) J. M. Parnis, G. A. Ozin, *J. Phys. Chem.* **1989**, 93, 4023; c) Z. L. Xiao, R. H. Hauge, J. L. Margrave, *J. Phys. Chem.* **1992**, *96*, 636.

[7] *Chemistry of Aluminium, Gallium, Indium and Thallium* (Ed.: A. J. Downs), Blackie, Glasgow, **1993**.

[8] N. J. Hardman, R. J. Wright, A. D. Phillips, P. P. Power, *Angew. Chem.* **2002**, *114*, 2966; *Angew. Chem. Int. Ed.* **2002**, *41*, 2842

[9] a) R. Ahlrichs, M. Bär, M. Häser, H. Horn, C. Kölmel, *Chem. Phys. Lett.* **1989**, *162*, 165; b) F. Weigend, M. Häser, *Theor. Chem. Acc.* **1997**, *97*, 331.

[10] A. Schäfer, C. Huber, R. Ahlrichs, *J. Chem. Phys.* **1994**, *100*, 5829.

[11] F. Weigend, M. Häser, H. Patzelt, R. Ahlrichs, *Chem. Phys. Lett.* **1998**, *294*, 143.

[12] Please order via email: andreas.koehn@chemie.uni-karlsruhe.de.

[13] T. Helgaker, H. J. A. Jensen, P. Jørgensen, J. Olsen, K. Ruud, H. Ågren, A. A. Auer, K. L. Bak, V. Bakken, O. Christiansen, S. Coriani, P. Dahle, E. K. Dalskov, T. Enevoldsen, B. Fernandez, C. Hättig, K. Hald, A. Halkier, H. Heiberg, H. Hettema, D. Jonsson, S. Kirpekar, R. Kobayashi, H. Koch, K. V. Mikkelsen, P. Norman, M. J. Packer, T. B. Pedersen, T. A. Ruden, A. Sanchez, T. Saue, S. P. A. Sauer, B. Schimmelpfennig, K. O. Sylvester-Hvid, P. R. Taylor, and O. Vahtras, DALTON—an electronic structure program, release 1.2, **2001**.

[14] A. Schäfer, H. Horn, R. Ahlrichs, *J. Chem. Phys.* **1992**, *97*, 2571.

[15] See, for example: a) J. A. Warren, G. R. Smith, W. A. Guillory, *J. Chem. Phys.* **1980**, *72*, 4901; b) M. E. Alikhani, B. Silvi, J. P. Perchard, V. Chandrasekharan, *J. Chem. Phys.* **1989**, *90*, 5221; c) M. E. Alikhani, L. Manceron, J. P. Perchard, B. Silvi, *J. Mol. Struct.* **1990**, *222*, 185.

[16] The calculations were carried out with the ASYM 40 program, version 3.0, upgrade of program ASYM 20, L. Hedberg, I. M. Mills, *J. Mol. Spectrosc.* **1993**, *160*, 117; If the atoms are numbered Ga1, H2, Ga3, H4, the choice of symmetry coordinates used in the analysis was: $S_1 = r(\mathrm{Ga1{-}H2}) + r(\mathrm{Ga1{-}H4}) + r(\mathrm{Ga3{-}H2}) + r(\mathrm{Ga3{-}H4})$, $S_2 = r(\mathrm{Ga1{-}Ga3})$, $S_3 = r(\mathrm{Ga1{-}H2}) - r(\mathrm{Ga1{-}H4}) + r(\mathrm{Ga3{-}H4}) - r(\mathrm{Ga3{-}H2})$, $S_4 = r(\mathrm{Ga1{-}H2}) + r(\mathrm{Ga1{-}H4}) - r(\mathrm{Ga3{-}H4}) - r(\mathrm{Ga3{-}H2})$, $S_5 = r(\mathrm{Ga1{-}H2}) - r(\mathrm{Ga1{-}H4}) - r(\mathrm{Ga3{-}H4}) + r(\mathrm{Ga3{-}H2})$, $S_6 = \tau(\mathrm{Ga1\text{-}H2\text{-}Ga3\text{-}H4})$.

[17] See, for example: H.-J. Himmel, A. J. Downs, T. M. Greene, *Chem. Rev.* **2002**, *102*, 4191.

[18] F. W. Froben, W. Schulze, U. Kloss, *Chem. Phys. Lett.* **1983**, *99*, 500.

[19] K. Balasubramanian, *J. Phys. Chem.* **1986**, *90*, 6786.

[20] T. K. Gosh, K. Tanaka, Y. Mochizuki, *Theochem.* **1998**, *451*, 61.

[21] K. K. Das, *J. Phys. B* **1997**, *30*, 803.

[22] G. Balducci, G. Gigli, G. Meloni, *J. Chem. Phys.* **1998**, *109*, 4384.

[23] I. Shim, K. Mandix, K. A. Gingerich, *J. Phys. Chem.* **1991**, *95*, 5435.

[24] K. P. Huber, G. Herzberg, *Molecular Spectra and Molecular Structure. IV. Constants of Diatomic Molecules*, van Nostrand Reinhold, New York, **1979**.

[25] S. Aldrige, Chem. Rev. **2001**, *101*, 3305. J. A. Pople, B. T. Luke, M. J. Frisch, J. S. Binkley, *J. Phys. Chem.* **1985**, *89*, 2198.

[26] a) K. Balasubramanian, *Chem. Phys. Lett.* **1989**, *164*, 231; b) C. W. Bock, K. D. Dobbs, G. J. Mains, M. Trachtman, *J. Phys. Chem.* **1991**, *95*, 7668.

[27] G. Treboux, J.-C. Barthelat, *J. Am. Chem. Soc.* **1993**, *115*, 4870.

[28] Y. Yamaguchi, B. J. DeLeeuw, C. A. Richards, Jr., H. F. Schaefer III., G. Frenking, *J. Am. Chem. Soc.* **1994**, *116*, 11 922.

[29] Z. Palágyi, H. F. Schaefer III, E. Kapuy, *Chem. Phys. Lett.* **1993**, *203*, 195.

[30] Similar arguments were used previously (see J. M. Parnis, G. A. Ozin, *J. Phys. Chem.* **1989**, *93*, 1220) to explain the reactivity of Al atoms toward H_2 and CH_4.

[31] For a general discussion of reaction mechanisms involving radicals see, for example: S. Shaik, A. Shurki, *Angew. Chem.* **1999**, *111*, 616, and references therein.

[32] The analysis of the ZPE contributions shows that the loss of ZPE for the H–H vibration (which mainly contributes to the imaginary mode) is compensated by the formation of Ga–H bonds.

Received: December 3, 2002 [F4633]

